Polymers for Advanced Technologies

WILEY

polymers advanced technologies

RESEARCH ARTICLE OPEN ACCESS

Modulation of Pectin Film Properties via Various Solid Lipid Nanoparticles Formulations: Water Barrier and Mechanical Insights

Mihaela Stefana Pascuta[1] | Verena Wiedenmann[2] | Dan Cristian Vodnar[1] | Ulrike Sabine van der Schaaf[3]

[1]Faculty of Food Science and Technology, Life Science Institute, University of Agricultural Sciences and Veterinary Medicine Cluj-Napoca, Cluj-Napoca, Romania | [2]Innovation Centre for Food and Process Technologies, Max Rubner-Institute, Federal Research Institute of Nutrition and Food, Karlsruhe, Germany | [3]Institute of Process Engineering in Life Sciences, Chair for Food Process Engineering, Karlsruhe Institute of Technology, Karlsruhe, Germany

Correspondence: Dan Cristian Vodnar (dan.vodnar@usamvcluj.ro) | Ulrike Sabine van der Schaaf (ulrike.schaaf@kit.edu)

Received: 13 February 2026 | **Revised:** 26 May 2026 | **Accepted:** 28 May 2026

Keywords: citrus pectin | dynamic mechanical analysis | edible film | water barrier | water sorption

ABSTRACT

Despite pectin-based films have been intensively studied as an alternative to plastic, their poor moisture barrier and mechanical properties remain challenging for researchers and industry. This study investigated the influence of four various solid lipid nanoparticles (SLN) formulations on pectin films. Their physical, mechanical, thermal, and morphological properties were tested to determine the functionality as active food packaging. Unloaded and rosemary oil-loaded pectin-stabilized SLN and Tween 20-stabilized SLN were characterized by size (between 140 and 436 nm), zeta potential (between −50 and −28 mV), and encapsulation efficiency (93.6% and 82.6%). SEM results exhibited the compatibility between pectin and SLN. The addition of SLN decreased the water vapor permeability (up to 92%), water uptake at 0.84 a_w (up to 37%), moisture content (up to 20%), and tensile strength (up to 74%) of pectin films. No significant change for the elongation at break was observed, compared to Control, in all developed pectin-based films ($p > 0.05$). Dynamic mechanical analysis showed a more elastic than viscous behavior of films between 30°C and 90°C. In vitro antimicrobial assay of pectin/rosemary oil-loaded SLN showed limited effect under *Escherichia coli, Salmonella enterica,* and *Staphylococcus aureus*. Pectin/SLN films immediately disintegrated in water. In conclusion, the present study indicates that the developed pectin/SLN films represent a promising preliminary approach as innovative and sustainable packaging materials intended for dried foods, while further studies are required to validate their suitability as a food-contact packaging system.

1 | Introduction

Food-grade biopolymers such as hydrocolloids (polysaccharides and proteins) can form edible films. For instance, pectin is a food-grade and biodegradable polysaccharide with versatile chemical and physical properties, for example, gelling [1] and emulsifying properties [2]. The gelling properties of pectin can be exploited to produce edible films suitable for food packaging [3]. Pectin films have been shown to form an excellent barrier to oil, aroma, and oxygen [4]. Despite their benefits, the low moisture barrier and poor mechanical resistance [1] are the main disadvantages. Pectin films can be further functionalized by incorporating lipids to reduce their weaknesses [5].

Lipids are often used as hydrophobic fillers to develop hybrid hydrocolloid films with increased moisture barrier while impacting other film properties (e.g., tensile, optical, and structural) [6, 7]. Despite the addition of lipids being a typical strategy to reduce the high hydrophilicity of the hydrocolloid films and sterically hinder the migration of water molecules through the film

[1], generally, its efficacy depends on (i) the hydrophilic–hydrophobic balance of the film constituents, (ii) the lipid distribution in the hydrocolloid matrix, considering the size of the droplets [6], and (iii) the state of the lipid, that is solid (crystalline) or liquid [8].

Essential oils (EO) are aromatic and volatile liquid oils usually extracted from plant material. EO are highly exploited as bioactive compounds in edible films, due to the growing demand for natural products. For instance, rosemary essential oil (RO) contains complex volatile compounds, especially monoterpenes such as eucalyptol and camphor, which have antimicrobial and antioxidant bioactivity. Therefore, RO is considered a promising natural food additive to replace synthetic preservatives [9]. EO are mixtures of numerous chemical compounds that influence their hydrophobicity, thus affecting their efficacy in reducing water vapor permeability. The effects of EO on the mechanical properties of hydrocolloid films are rather unpredictable due to their complex composition, which interacts differently with the biopolymeric network. Depending on the characteristics of the EO added into the film matrix, EO might induce heterogeneity in the film structure featuring discontinuities, thus reducing the tensile properties [6]. However, the direct incorporation of EO into hydrocolloid films often leads to unacceptable packaging material performance, resulting in poor storage stability/loss of initial properties due to EO volatility release. One approach to overcome this issue is the nanoencapsulation of EO into a proper nanocarrier. Solid lipid nanoparticles (SLN) are suitable nanocarriers for hydrophobic compounds such as EO that may protect them and offer them a controlled release [10], thus improving the functionality of films [11].

SLN are crystallized, nanoscale lipid particles. The fat phase generally consists of solid lipids stabilized by one or more emulsifiers [12]. Lipids and emulsifiers are extrinsic factors that affect the properties of pectin-based gels. Solid oils increase the strength of gels compared to liquid oils [13]. Recently, it was demonstrated that beeswax-based SLN improved the structural integrity of plantain peel pectin films [14]. Non-ionic emulsifiers such as Tween 20 and Tween 80 represent inactive fillers, while biopolymeric-based emulsifiers represent active fillers for gel formulation. -In the previous study, it was shown that protein-stabilized SLN as active fillers reinforced the protein gel network, whereas Tween 20-stabilized SLN as inactive fillers weakened the protein gel network. Furthermore, the properties of protein films were modulated by using SLN as active/inactive fillers. Active and inactive fillers had different impacts on the mechanical properties of protein films. Active fillers became an integrative part of the film matrix, thereby not influencing films' mechanical properties. Instead, inactive fillers caused higher molecular mobility due to the plasticizer effect of Tween 20 and the formation of incomplete pores, thus weakening the films' mechanical properties [12]. When SLN were loaded with active EO compounds (cinnamaldehyde, eugenol, and thymol), they also did not affect the ultimate tensile strength of pullulan films [15]. However, the modulation of mechanical properties of hydrocolloid films by using SLN needs further research to elucidate their action by solid lipid and emulsifier type, loaded/unloaded SLN, and hydrocolloid matrix.

Crystalline lipids provide a better barrier to moisture transport than liquid lipids [8] since they act as an impermeable dispersed phase and can reduce mass transfer due to increased tortuosity of the diffusional path [16]. Triglyceride-based SLN are platelet-shaped particles that may produce a tortuous path into the film matrix, reducing water vapor diffusion across the films. SLN as both active and inactive fillers reduced the WVP of β-lactoglobulin films [12]. Beeswax-based SLN also reduced the WVP of plantain peel pectin films [14]. Due to the limited literature on the SLN action in reducing the WVP of hydrocolloid films, further research is required.

Recent studies have investigated rosemary oil as a filler in pectin [17] or other biopolymeric-based films [18]. SLN was used as a nanocarrier for EO in edible alginate coatings [19] and in chitosan/polyvinyl alcohol hydrogels [20]. To our knowledge, the exact synergy of all these components—pectin/rosemary oil/solid lipid nanoparticles as a solid matrix/film—regarding water vapor permeability and mechanical properties has not been exploited. Furthermore, since pectin has both gelling and emulsifying properties, it was considered whether the previous protein-based system [12] is appropriate and transferable to a pectin-based system.

This study hypothesizes that incorporating rosemary oil–loaded solid lipid nanoparticles (RO-SLN) into pectin films will improve their water barrier performance by valorising the crystalline lipid phase and platelet-like shape nanoparticles to create a tortuous diffusion path. Furthermore, the mechanical properties of the pectin films can be modulated by employing rosemary oil-loaded SLN as either active or inactive fillers, determined by the emulsifier used for RO-SLN stabilization. Therefore, SLN were stabilized either by pectin (PS) or by Tween 20 (TS) as active/inactive fillers for the pectin films. Consequently, pectin/rosemary oil-loaded SLN films (PS-RO and TS-RO) were compared to: (i) pectin films with unloaded SLN (PS and TS); (ii) pectin/emulsifier films without any lipids (CPS and CTS); and (iii) films with free rosemary oil (CRO). All pectin films were characterized by their mechanical, thermal, morphological, and water barrier properties. The in vitro antimicrobial activity of the formulated film-forming solution was also provided as a first step towards bioactive packaging materials.

2 | Materials and Methods

2.1 | Materials

Citrus pectin (CU-L 103/21) with a 45% degree of methoxylation (DM) and 88% galacturonic acid was kindly donated by Herbstreith & Fox GmbH & Co (Neuenburg, Germany). Soy lecithin, "Emulpur IP," was donated by Cargill Texturizing Solutions (Hamburg, Germany). Tristearin was procured from IOI Oleo GmbH (Hamburg, Germany). Sucrose palmitate was purchased from Alfa Aesar, ThermoFisher GmbH (Karlsruhe, Germany). Tween 20 (Polyoxyethylene sorbitan monolaurate) was procured from Sigma Aldrich (St. Louis, Missouri, USA). Glycerol (glycerin 99.5%) was purchased from Analar Normapur, BDH Prolabo (München, Germany). Rosemary oil (Rosmarinoel Aroma nat.) was obtained from Symrise

(Nördlingen, Germany). Calcium chloride ($CaCl_2$) granulate, potassium carbonate (K_2CO_3), sodium chloride (NaCl), potassium acetate (CH_3COOK), magnesium nitrate hexahydrate ($Mg(NO_3)_2$), magnesium chloride ($MgCl_2$), and potassium dihydrogen phosphate were procured from Carl Roth GmbH + Co (Karlsruhe, Germany). $CaCl_2$ dihydrate, lithium chloride (LiCl), sodium bromide (NaBr), potassium chloride (KCl), and disodium hydrogen phosphate dihydrate were purchased from Merck KgaA (Darmstadt, Germany). All solutions were prepared in demineralized water.

2.2 | Preparation of SLN

SLNs were prepared by ultrasound-assisted hot emulsification [12]. Emulsifier solutions were prepared in 5 mM phosphate buffer at pH 7.0 (w/w): 3.02% sucrose palmitate solution and 8% Tween 20 solution. Then, a 2% (w/w) pectin solution was prepared by dissolving pectin in hot distilled water (90°C) using an Ultraturax T25 basic (IKA—Werke) at 9500 rpm for 5 min, followed by an increased speed to 17,500 rpm for another 5 min. The solution was kept at room temperature until use.

The emulsion for each SLN batch was prepared as follows: 0.125 g soy lecithin and 2.5 g tristearin were heated under stirring to 80°C for 30 min to remove any crystal memory. For RO encapsulation, 0.5 g RO was stirred with melted lecithin and tristearin at 80°C for 1 min. Then, 22.375 g of sucrose palmitate solution (80°C) was added to the melt. The mixture was emulsified by ultrasonic homogenization for 30 min using a sonicator (Sonoplus HD 3100, Bandelin electronic GmbH, Berlin, Germany) with a titanium tip (VS70T) at an amplitude of 75% in pulsed mode (0.5 s pulse length). During emulsification, a thermostated water bath (Lauda Alpha RA 8, Germany) was used to maintain a temperature of 60°C for 30 min, especially for better pectin adsorption onto the surface of the SLN [21].

Hot emulsions with or without RO were poured into Tween 20 and pectin solution (60°C) in equal amounts, followed by a vortex step at 2500 rpm for 20 s and immediately cooled down to 20°C in an ice bath under continuous stirring. The composition of SLN is given in Table 1 [21]. To remove the abraded titanium particles during sonication, SLN were centrifuged at 3220 × *g*, 25°C for 10 min (Eppendorf Centrifuge 5810 R, Germany). Pectin-stabilized SLN were diluted with distilled water to reduce viscosity before centrifugation. The dilution ratio was 1:4 (w/w) water to emulsion.

2.3 | Preparation of Pectin-Based Films

Pectin films were produced using the casting method [22] with modifications. For obtaining film-forming solution (FFS), hot distilled water (90°C) was added to the beaker containing glycerol and was homogenized with an Ultraturrax T25 basic at 9500 rpm for 30 s. Then, pectin was gradually added during homogenization at 9500 rpm for 5 min, and the speed was then increased to 17,500 rpm for another 5 min. FFS (60°C) and SLN (25°C) were homogenized using the Ultraturrax at 9500 rpm for 2 min. $CaCl_2$ solution was added to the film mixture during this homogenization. Then, an ultrasonic bath (Bandelin Sonorex Digitec, DT 100 H, 35 kHz, Germany) was used to remove air bubbles (42°C ± 1°C, 30 min). The film mixture was immediately poured into polyethylene Petri dishes (diameter of 9 cm) coated with Teflon foil. To ensure the same thickness in all films, the dry mass per cm^2 was kept constant at 0.01 g/cm^2. Films were dried at 25°C ± 1°C and 55% relative humidity (RH) for 6 days before film characterization. In addition to pectin/rosemary oil-loaded SLN films (PS-RO and TS-RO) and pectin/unloaded-SLN films (PS and TS), different control films were produced: pectin/emulsifier films that are required to stabilize SLN, but no fat phase (CPS and CTS); pectin/free RO films (CRO); and pectin films without no addition (Control). The composition and the dry mass of film mixtures are presented in Table 2. At least three replicates ($n = 3$) were produced for each type of pectin film.

2.4 | SLN Characterization

2.4.1 | Size and Zeta Potential

A ZetaSizer (Malvern Instruments, UK) was used to measure both the size and zeta potential of SLN [12], with slight modifications. 0.5 g SLN were diluted in 18 mL distilled water, then the conductivity was adjusted to 45 ± 2 $\mu S \cdot cm^{-1}$. Before analysis, the dilutions of PS and PS-RO were filtered using Minisart NML syringe filters (1.2 μm, 28 mm, Carl Roth GmbH + Co, Karlsruhe, Germany) to remove undissolved pectin particles. Zeta potential (ZP) was measured via the electrophoretic mobility of the particles. The particle size was measured by dynamic light scattering at 25°C. The backscattered light was collected at 173°. The *z*-averages were analyzed based on the intensity-based particle size distributions using the Mie theory.

TABLE 1 | Solid lipid nanoparticles composition (%).

SLN	Lecithin	Tristearin	Sucrose palmitate	Rosemary oil	Tween 20	Pectin
PS	0.25	5	1.35	—	—	1
PS-RO		4		1	—	1
TS		5		—	4	—
TS-RO		4		1	4	—

Abbreviations: PS, pectin-stabilized solid lipid nanoparticles; PS-RO, rosemary oil loaded pectin-stabilized solid lipid nanoparticles; SLN, solid lipid nanoparticles; TS-RO, rosemary oil loaded Tween 20-stabilized solid lipid nanoparticles; TS, Tween 20-stabilized solid lipid nanoparticles.

TABLE 2 | The composition and the dry mass of film mixtures.

	Composition/%		Dry mass/%							
Films	Pectin solution	SLN	Lecithin	Tristearin	Sucrose palmitate	RO	Tween 20	Glycerol	$CaCl_2$	Pectin
PS	60	40	0.1	2	0.5	—	—	0.5	0.02	1.8
PS-RO	60	40		1.6		0.4	—			
CPS	60	—		—		—	—			
TS	60	40		2		—	1.6			
TS-RO	60	40		1.6		0.4				
CTS	60	—		—		—				
CRO	100	—	—	—	—	0.4	—			
Control	100	—	—	—	—	—	—			

Abbreviations: control, pectin film; CPS, pectin/emulsifier used in PS (lecithin and sucrose palmitate) film; CRO, pectin/rosemary oil film; CTS, pectin/emulsifier used in TS (lecithin, sucrose palmitate, Tween 20) film; PS, pectin/pectin-stabilized SLN film; PS-RO, pectin/rosemary oil-loaded pectin-stabilized SLN film; SLN, solid lipid nanoparticles; TS, pectin/Tween 20-stabilized SLN film; TS-RO, pectin/rosemary oil-loaded Tween 20-stabilized SLN film.

2.4.2 | Encapsulation Efficiency

The ultrafiltration/centrifugation technique determined the free RO and the encapsulation efficiency (EE), which was calculated according to [23]. The filtration units (Vivaspin 2, membrane 300.000 MWCO PES, Sartorius, Germany) were prewashed, filled with 2 g of the sample, and centrifuged (Eppendorf Centrifuge 5810 R, Germany) for 2 × 30 min at 3220 × *g* (20°C). The filtrate was diluted with pure ethanol (1:1 v/v) and vortexed for 20 s. The absorbance of the mixed solution was measured at 275 nm (λ_{max}). The amount of free RO was calculated using an RO calibration curve in the range of 0.3 to 5 mg/g at the wavelength of 275 nm ($R^2 = 0.999$), performed with the UV–VIS spectrophotometer (Varian Cary 50 Scan, Software Version 02.00/25). The EE was calculated using the following equation:

$$EE(\%) = \frac{RO_T - RO_F}{RO_T} \times 100 \quad (1)$$

where EE was the encapsulation efficiency, %; RO_T was the theoretical (total) amount of rosemary oil, mg; and RO_F was the free amount of rosemary oil, mg.

In vitro antimicrobial analysis of film-forming solution containing pectin solution and SLN nanoemulsion is discussed in the Supporting Information. The antimicrobial activity against *Escherichia coli, Salmonella enterica*, and *Staphylococcus aureus* is represented by Figure S1.

2.5 | Characterization of Films

2.5.1 | Water Disintegration

The water disintegration of films was visually evaluated, and their disintegration was appreciated. Distilled water was used as a food simulant (mimicking aqueous foods). Rectangular pieces (1 × 4 cm) of each film were immersed in 25 mL of distilled water under gentle stirring.

2.5.2 | Scanning Electron Microscopy (SEM)

For the morphological SEM analysis, a small piece of approximately 1.5 cm^2 was ripped from each film sample and mounted on an adhesive and conductive support tab, deposited on an aluminum stub (Plano, Germany). To reduce charging, the film samples were sputtered with platinum in Argon atmosphere (30 s coating at ca. 5–10 mA current). Imaging was carried out with a Quanta 250 FEG field emission scanning electron microscope (FEI, Brno, Czech Republic) under high vacuum conditions (~3×10^{-7} mbar) with an Everhart–Thornley detector, a working distance of 5 mm, and an accelerating voltage of 10 kV. Besides a top view on the surface morphology of each film, a side view of the inner film structure could be visualized at the ripped sample edges.

Optical properties of pectin/rosemary oil-loaded films are discussed in the Supporting Information. The opacity of pectin-based films is presented in Figure S2.

2.5.3 | Water Sorption Isotherms and Moisture Content

Water sorption was determined by gravimetric analysis. 2 cm^2 of sample were transferred into 8 desiccators containing various saturated salt solutions to 25°C (water activity (a_w) = 0.11, LiCl; 0.23, CH_3COOK; 0.33, $MgCl_2$; 0.43, K_2CO_3; 0.53, $Mg(NO_3)_2$; 0.58, NaBr; 0.75, NaCl; 0.84, KCl). The mass gain (water uptake of the films) was periodically measured until the films were equilibrated. The water uptake was calculated as a percentage between the mass of the equilibrated film at a chosen a_w and the initial mass of the film at 0.55 a_w. All values were normalized with the 0.11 a_w sample. For clarity, water uptake of raw materials was calculated with the same formula, followed by the calculation of theoretical curves of films based on the water uptake contribution of each raw material.

For moisture content, two pieces (2 cm^2) of each solid film were weighed before and after drying to 102°C to reach a constant dry mass, and the result was expressed as a percentage.

2.5.4 | Water Vapor Permeability

Water vapor permeability (WVP) was determined according to ASTM E96/E96M-10 standard with a RH gradient of 0/75%. The films were sealed onto aluminum cups containing approximately 7 g of anhydrous $CaCl_2$, exposing 10 cm^2 of the film to water vapor and leaving a 6 mm air gap between the desiccant and the underside of the sample. The cups were placed into a controlled temperature (25°C ± 1°C) and RH (75% ± 1%) chamber (ESPEC, EX-111, Tabai Espec Corp.) and weighed seven times in 2 days. A linear regression ($R^2 < 0.997$) was made of the weight gain versus time. The slope was divided by the exposed area of the film to calculate the water vapor transmission rate (WVTR). For WVP, firstly, the water vapor partial pressure difference (WVPP) at the underside of the films was calculated using the Correction for Resistance due to Still Air and Specimen Surface equation as described in ASTM E96/E96M-10 standard. Then, WVP was calculated by multiplying the WVTR by the thicknesses of the films and dividing it by the WVPP between both sides. Mean values of five points per film were considered for the thickness (Table S1).

2.5.5 | Mechanical Properties

Mechanical properties analysis was adapted according to Siracusa, Romani, Gigli, Mannozzi, Cecchini, Tylewicz, and Lotti [24]. The tensile strength (TES) and elongation at break (EAB) were determined for all films. The films were preconditioned at 23°C ± 2°C and 55% RH. According to ASTM E96/E96M-10, ~50 × 10 × 0.09 mm of each sample type were tested with Zwick & Roell Z2.5 (grip 8201/2.5 kN, Ulm, Germany) D882-09 standard. An initial grip separation of 25 mm and a speed of 10 mm/min were applied. Software V11.02 directly calculated TES and EAB. Samples were analyzed in triplicate ($n = 3$).

2.5.6 | Dynamic Mechanical Analysis (DMA)

DMA was conducted according to Andrzejewski, Grad, Wiśniewski and Szulc [25] with a few modifications. DMA was performed with an Anton Paar MCR 301 rheometer with a CTD 450 oven equipped with torsion clamps (SRF 12). The storage modulus (G′) and loss modulus (G″) of samples (~40 × 10 × 0.09 mm) were determined at a frequency of 1 Hz and a strain amplitude of 0.1%. The temperature was increased by 2°C/min from 30°C to 90°C. The final curves are the result of averaging two replicates ($n = 2$), where the error bars are not shown for clarity.

2.6 | Statistical Analysis

Statistical analysis and graphs were performed in Microsoft Excel 2016 at a confidence level of 95%. All experiments were run in triplicate unless otherwise stated. Results were expressed as mean value ± standard deviation (SD). Descriptive analysis was performed for all measurements before further tests. The Fmax test was used to analyze the homogeneity of data. For homogeneous data, one way ANOVA test with the *post hoc* Scheffe test was applied. For heterogeneous values, the Fmax test was applied to check homogeneity between every two groups before applying the *t*-test. Both *t*-test assuming unequal variances (for heterogeneous data) and *t*-test assuming equal variances (for homogeneous data) were used. Letters were used to express significant differences.

3 | Results and Discussion

3.1 | Characterization of SLN

In order to characterize SLN, particle size, polydispersity index (PdI), and ZP of unloaded (PS and TS) and loaded (PS-RO and TS-RO) SLN were determined (Table 3). Furthermore, EE was analyzed for loaded SLN. These are essential parameters for the film's properties, as the particle characteristics determine their integration in the films and the latter film [26, 27]. The particle sizes of PS and TS were 402 ± 42 and 179 ± 4 nm, respectively. Although pectin and Tween 20 were adsorbed to the particle surface, the larger size of PS compared to TS may be attributed to the larger pectin. An increased size of solid lipid nanoparticles by adding pectin: the sizes ranged from 210 to 370 nm after pectin addition, compared to a size of 150 to 230 nm before adding pectin [28]. The particle size of PS-RO and TS-RO was 436 ± 102 and 140 ± 2 nm, respectively. The addition of RO decreased the size of TS-RO. One reason for this size reduction could be a change in shape. Additionally, a reduced particle size and PdI of loaded SLN compared to unloaded ones was previously described for *Ridolfia segetum* EO [29] and *Croton argyrophyllus* Kunth EO [30]. It was supposed that the introduction of EO in the lipid matrix to support the nanostructuring effect promoted by the lipophilic nature of EO [29]. In contrast to that, the addition of RO did not significantly influence the size of PS-RO ($p > 0.05$). The contribution of the pectin adsorption to the size of PS and PS-RO is much larger than that of the actual SLN-core. Therefore, size changes caused by changes in the SLN shape are not statistically relevant to the overall size of PS and PS-RO. The PdI values of SLN were between 0.23 ± 0.01 (TS-RO) and 0.33 ± 0.01 (PS-RO) indicating relatively narrow size distributions and thus uniform particle shapes.

Moreover, ZP is a critical factor in evaluating a colloidal system's stability by indicating the net surface charge. The ZP

TABLE 3 | Particle size (nm), polydispersity index (PdI), zeta potential (ZP), and encapsulation efficiency (EE) of SLN.

SLN	*z*-average (nm)	PdI	ZP (mV)	EE (%)
PS	402 ± 42^{b}	0.32 ± 0.01^{a}	-46 ± 1^{b}	—
PS-RO	436 ± 102^{a}	0.33 ± 0.01^{a}	-50 ± 3^{c}	93.6 ± 0.1^{a}
TS	179 ± 4^{c}	0.29 ± 0.01^{ab}	-28 ± 1^{a}	—
TS-RO	140 ± 2^{d}	0.23 ± 0.01^{b}	-28 ± 1^{a}	82.6 ± 3.9^{b}

Note: Data are expressed as mean ± SD ($n = 9$). Letters represent significant differences ($p < 0.05$).
Abbreviations: PS, pectin-stabilized solid lipid nanoparticles; PS-RO, rosemary oil loaded pectin-stabilized solid lipid nanoparticles; SLN, solid lipid nanoparticles; TS, Tween 20-stabilized solid lipid nanoparticles; TS-RO, rosemary oil loaded Tween 20-stabilized solid lipid nanoparticles.

for PS and TS was −46 ± 1 and −28 ± 1 mV, respectively. The more negative surface charge of PS was presumably due to the adsorbed pectin that contains carboxyl groups (–COOH) in its molecular structure. pH values higher than 3.5 (pK_a of pectin) lead to a dissociation of –COOH, thus leading to an increased negative surface charge and a more negative ZP [31]. A higher ZP of pectin-stabilized SLN was also confirmed by [32]. RO-loaded SLN decreased the ZP of PS-RO to −50 ± 3 mV while maintaining a ZP value of −28 ± 1 in TS-RO. Depending on the loaded EO type, stronger adsorption of anionic pectin at the oil surface may occur, thus resulting in more negative ZP and higher stability of the SLN. A higher adsorbed content of pectin may improve the electrostatic repulsive forces between particles. A different ZP was observed for EO-loaded nanoemulsions with pectin [33]. In all produced SLN, ZP was close to −30 mV or even more negative. ZP values of 30 or more are generally indicators of stable suspensions/emulsions [34]. Thus, the prepared SLN types are also assumed to prove stable.

SLN are able to encapsulate hydrophobic compounds such as EO with high EE, even close to 100% [10, 35, 36]. PS-RO and TS-RO had an EE of 93.61% ± 0.11% and 82.55% ± 3.87%, respectively. The higher EE in PS-RO may be attributed to pectin's high viscosity and rapid gel-forming ability that led to a stronger gel matrix and therefore, to optimum RO entrapment [37]. Overall, the obtained EE values are comparable to those reported for other SLN nanocarriers with encapsulated EO: *Zataria multiflora* EO [35], *Satureja khuzistanica* EO [38], and *Ziziphora clinopodioides* EO [39], which were entrapped in the SLN, had EE of 84% ± 0.92%, 84.5%, and 93%, respectively.

3.2 | Characterization of Pectin Films

3.2.1 | Water Disintegration

The water disintegration of the films mimics the profile of films if applied in humid environments or on the surface of foods with high water content [40]. The water disintegration of films was observed immediately after immersion in distilled water, as presented in Figure 1. The water-soluble property of pectin films was not affected by insoluble SLN addition despite the increased amount of insoluble matter (lipids). Pectin/SLN films were disintegrated entirely in water. Additionally, after complete disintegration of the SLN-containing films without any visible lumps, it could be noticed that the solutions remained turbid. The turbidity was caused by the SLN, now dispersed in water. This result indicates that the SLN remained sufficiently stabilized by their respective emulsifier system even after strong dilution. On the other hand, under gentle agitation, Control was wholly dissolved in water without any trace of residuals. Pectin/glycerol films developed by [41] and carrageenan/Tween emulsifier films produced by [42] also showed complete solubility in water. Pectin has a highly hydrophilic nature due to the presence of hydroxylic groups (–OH) in its chain that favor the adsorption of water molecules, thus forming more hydrogen bonds in the pectin matrix. Therefore, pectin/SLN films may be suitable for application as edible bags for dried food instead of wet food [43]. Alternatively, pectin/SLN films could be consumed with ready-to-eat food products, if the water contained in the food product is evaporated through the cooking process (e.g., fried/grilled meat).

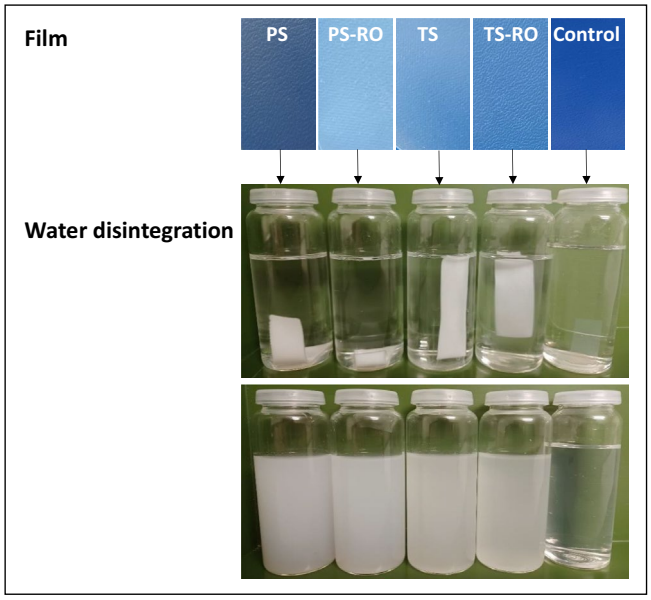

FIGURE 1 | Water disintegration of pectin/SLN films.

3.2.2 | Scanning Electron Microscopy (SEM)

The morphological aspect was studied to gain information on the organization of SLN throughout the matrix of the films. The SEM micrographs of the surfaces and internal structure of the films are shown in Figure 2. The surface of pectin/SLN films appeared to be rougher than the Control. Their surface appeared flat, smooth, and compact, rather than featureless, which corresponds to pectin films developed by [44–46]. Meanwhile, the side view of the ripped edges showed a layered internal structure of the Control. The addition of SLN interrupts the layer formation and leads to a less regular structure of film matrices. However, the SLN were assimilated entirely and well distributed in the matrix without causing irregularities, and no areas of phase separation could be observed. SLN themselves are too small to be observed with the given magnification; larger SLN agglomerates could not be seen. Therefore, pectin/SLN films showed good miscibility, suggesting a favorable interaction among the components of these formulations. Overall, SEM images show that SLN were very well incorporated into the pectin film matrix, leading to homogeneous films with a more pronounced microstructure compared to the Control films.

3.2.3 | Water Sorption Isotherm and Moisture Content

Water sorption was determined at gradually increased water activity (a_w) to analyze the sensitivity of pectin films to water vapor (Figure 3). The water uptake in pectin/SLN films significantly ($p < 0.05$) decreased compared to Control and pectin/emulsifier films. The water uptakes at 0.84 a_w were between 17.93% ± 2.88% (PS-RO) and 33.84% ± 1.07% (CRO). CRO film had the highest value of water sorption, but this was not significantly different from that of the Control ($p > 0.05$).

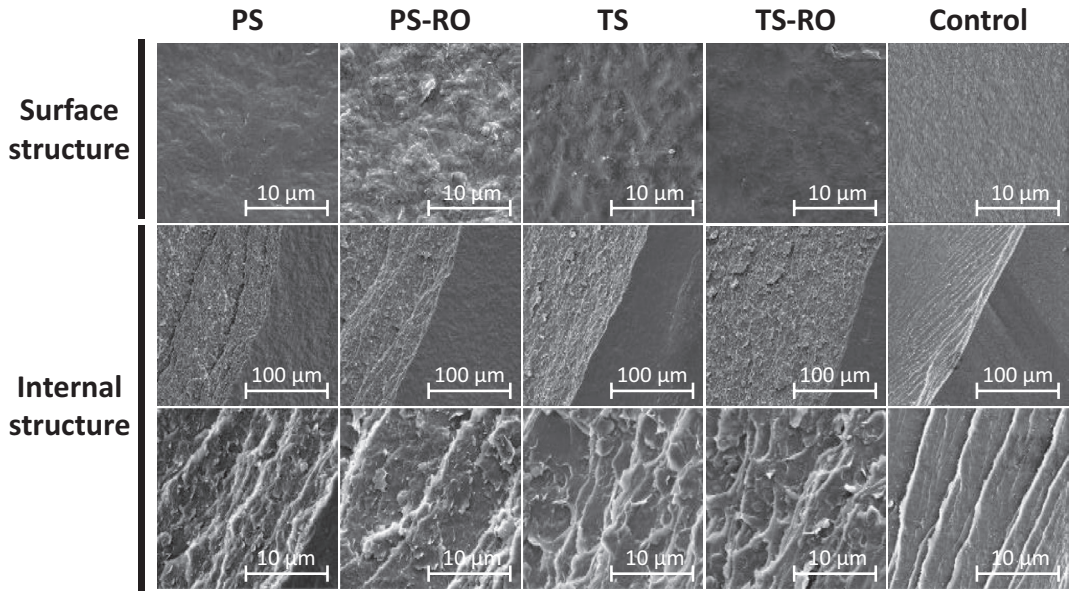

FIGURE 2 | Scanning electron microscopy images of pectin/SLN films.

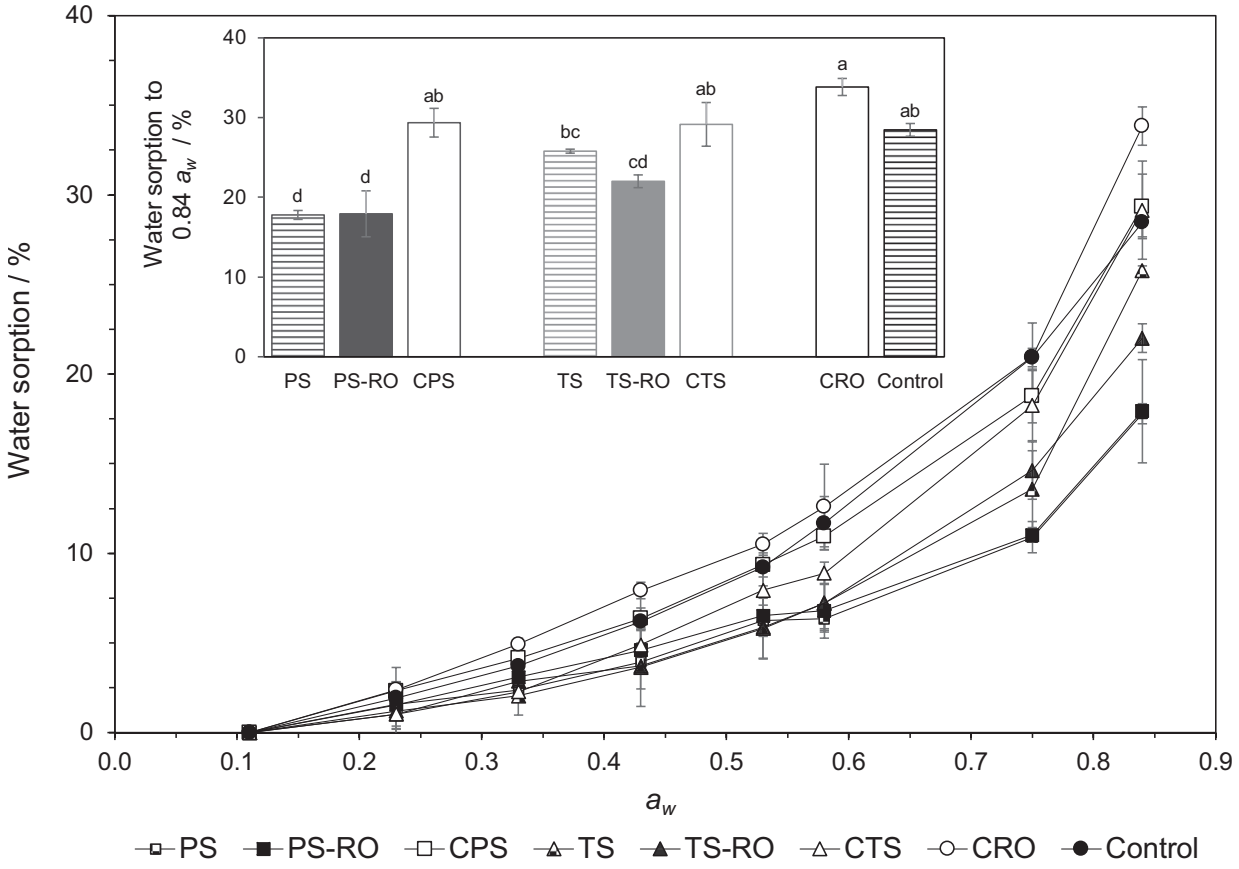

FIGURE 3 | Water sorption of pectin films. Data are expressed as mean ± standard deviation ($n = 3$).

Additionally, no significant differences in water sorption could be observed between PS and PS-RO or between TS and TS-RO, respectively ($p > 0.05$). The shapes of all water sorption isotherms were typical for hydrophilic substances. The water uptakes increased with increasing a_w, with a steep rise after around 0.60 a_w. At a lower a_w, water sorption increased slowly due to reduced water-binding sites at the surface of films. As a_w increased, the films started to swell, and the water-binding sites were better accessible [47].

Two aspects may influence the water sorption of the films: Firstly, by synergistic effects between raw materials. For instance, a synergistic effect appeared between glycerol and surfactants (Tween 20, Span 80, and lecithin) in starch films. Their

combination enhanced the absorption of water molecules [48]. To see if synergistic effects were present, theoretical water sorption isotherms were calculated and compared to the measured ones (Figure S3). The theoretical ratios were calculated based on each raw material's water sorption contribution (Figure S4). The theoretical curves correlated well with the measured ones, indicating that the raw materials dominated the water sorption and no synergistic effects occurred.

A further reason for high water sorption is the film composition. Hydrophilic substances such as pectin, glycerol, and $CaCl_2$ have high water sorption in humid environments. The higher the amount of hydrophilic materials in films, the higher the water sorption percentage. The variation of pectin/glycerol/$CaCl_2$ content in each film can impact the water sorption. In order to examine the share of hydrophilic raw materials in the water sorption, the results were correlated with the films' pectin/glycerol/$CaCl_2$ content (Figure S5). The hydrophilic fractions correlated well with the water uptake at 0.84 a_w ($R^2 = 0.675$). These hydrophilic raw materials were partially replaced by SLN containing tristearin and emulsifiers. The lipophilic tristearin did not contribute to water sorption; thus, the reduced water sorption of pectin/SLN films was probably due to a lower amount of pectin/glycerol/$CaCl_2$. These results are in good accordance with the results that indicated that the water sorption was dominated by the raw materials and not by interactions between the materials.

The moisture content of pectin films ranged between 14.15% ± 1.12% (PS) and 20.77% ± 0.99% (CTS) (Figure 4). Pectin/SLN films had significantly lower moisture content values than pectin/emulsifier films and Control ($p < 0.05$). In the case of water sorption isotherms, the decrease in moisture content was also attributed to the ability of raw materials to bind water. The hydrophobic tristearin found in SLN partially replaced the highly hydrophilic materials (pectin, glycerol, and $CaCl_2$), thereby decreasing the moisture content of pectin/SLN films. The hydrophilic part of emulsifiers maintained an increased moisture content in pectin/emulsifier films without significant differences compared to the Control ($p > 0.05$). Emulsifiers contain both hydrophilic and lipophilic components, and their ability to bind water depends on the Hydrophilic–Lipophilic Balance. Since Tween 20 has a high HLB of 16.7, it is considered a hydrophilic emulsifier [49] that could explain the highest moisture content in CTS film. A similar result was reported when fatty acids were added to pea starch-guar gum films [50]. RO did not influence the moisture content, agreeing with the results obtained from water sorption.

3.2.4 | Water Vapor Permeability

WVP is an important factor for evaluating the water barrier properties of films and their application in food packaging. A lower WVP is highly desirable to prevent moisture transfer between food and the external environment. Therefore, the lower the WVP, the higher the water vapor barrier. This leads to an increased quality of packaged food and extends the food shelf life [51]. WVP is shown in Figure 5.

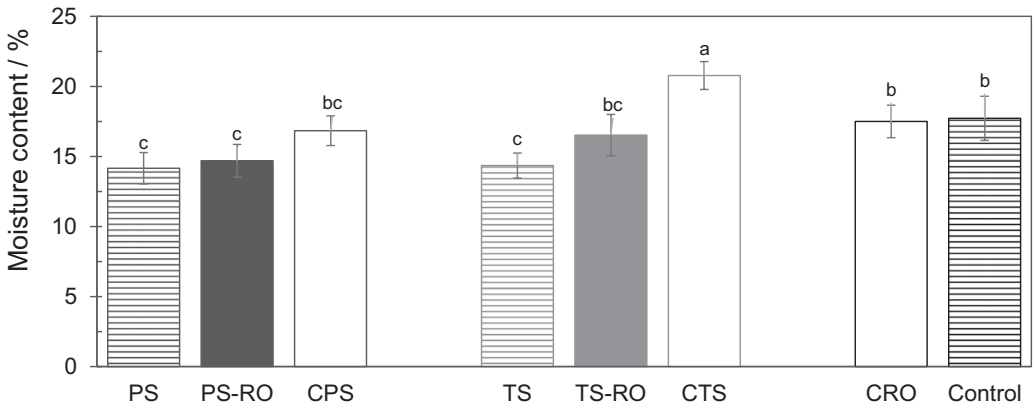

FIGURE 4 | Moisture content of pectin films. Data are expressed as mean ± standard deviation ($n = 3$).

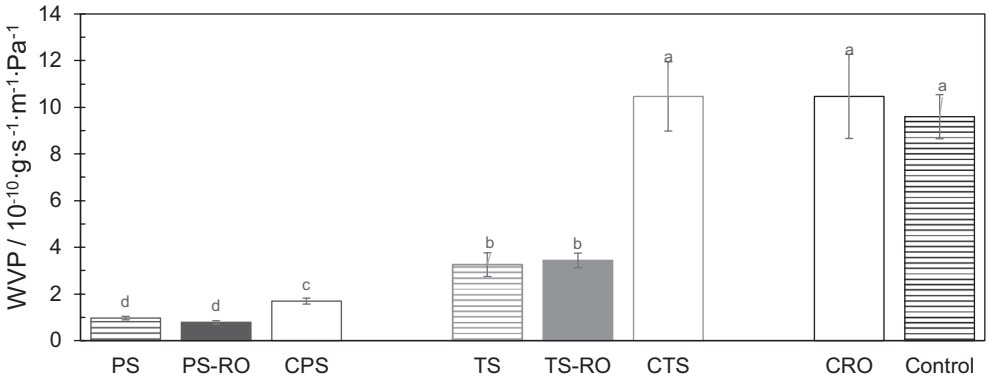

FIGURE 5 | Water vapor permeability (WVP) of pectin films with differently stabilized solid lipid nanoparticles (SLN) that were unloaded or loaded with rosemary oil. Data are expressed as mean ± standard deviation ($n = 3$).

WVP was found to be in the range of 0.78 ± 0.07 to $10.47 \pm 1.80 \times 10^{-10}$·g·m^{-1}·s^{-1}·Pa^{-1}. No statistical differences between CRO, CTS, and Control were observed ($p > 0.05$). Loading RO into the films did not significantly influence the WVP ($p > 0.05$), neither when incorporated within the SLN nor when directly added into the film matrix. This result is well correlated to the above-mentioned water sorption isotherms and moisture content. However, pectin/SLN films had the lowest WVP, up to 92% lower value than the Control in PS-RO. Emulsifiers influenced the WVP: lecithin and sucrose palmitate significantly decreased ($p < 0.05$) the WVP as seen in the CPS (films containing added lecithin and sucrose palmitate but no lipids), while the presence of Tween 20 in the CTS film maintained an increased WVP.

This study hypothesized that SLN might reduce the WVP for several reasons: (I) Considering previous work [12, 52, 53], SLN are nanoparticles with a platelet shape, thus having a large aspect ratio. Due to this large aspect ratio, platelet-like particles are a better obstacle to water molecules diffusing through the film than the same volume fraction of spherical particles [54, 55]. This can be the reason why the WVP is much lower in all the SLN-containing films compared to their controls. (II) SLN are crystalline lipid particles, thus lowering the WVP probably more effectively than liquid lipid droplets at comparable volumes [8, 56]. This may also be the reason why the WVP of films with free RO did not show a significant difference compared to the controls: RO is a liquid lipid at room temperature, which, when not loaded in SLN, was present as spherical droplets with $142 \pm 20\,\mu$m in size (D90,3). In contrast, when RO is loaded in SLN, the effect of tristearin dominates. Tristearin appeared as crystalline particles whether or not RO was incorporated, explaining why there was no difference between the WVP of PS and PS-RO as well as between TS and TS-RO. (III) Tristearin, lecithin, and sucrose palmitate, the main ingredients of SLN, have a hydrophobic part that could affect the hydrophilic/hydrophobic character of films, as can also be seen in Section 3.2.4. If the films become more hydrophobic due to the presence of the SLN, the WVP decreases since water vapor transfer often occurs through the hydrophilic part of the film [57]. Pectin/SLN films had more hydrophobic parts per g dry mass since SLN partially replaced hydrophilic portions of the pectin network, as other studies showed [12].

Emulsifiers probably influenced WVP due to their hydrophobic parts and homogenous distribution within the films. In earlier work, it has been shown that sucrose palmitate and lecithin reduced the WVP of protein films [12]. This WVP-reducing effect of sucrose palmitate and lecithin can be seen in CPS. In contrast, Tween 20 has a very hydrophilic nature that compensates WVP, reducing the effect of sucrose palmitate and lecithin and resulting in the same WVP as the Control. Therefore, this could also explain the higher WVP in TS and TS-RO compared to PS and PS-RO. Ziani, Oses, Coma, and Maté [58] observed an increased WVP in chitosan films by incorporating Tween 20 and glycerol. A very low WVP characterizes conventional plastic films. For instance, a WVP of about 2×10^{-12}·g·m^{-1}·s^{-1}·Pa^{-1} was reported for polyethylene films [59] and 4.5×10^{-11}·g·m^{-1}·s^{-1}·Pa^{-1} for polypropylene films [60]. However, by incorporating RO-loaded SLN, it was possible to reduce WVP by almost an order of magnitude, making it a suitable approach to improve the water barrier of pectin films. SLN are crystalline and hydrophobic particles in the nanoscale range with a platelet-like shape that may reduce water uptake, thus supporting the improvement of the moisture barrier.

3.2.5 | Mechanical Properties

Mechanical properties provide information about the resistance of films to certain stress during handling, transport, and processing. Tensile strength (TES) and elongation at break (EAB) were determined for all pectin films to better understand these properties. TES shows the tensile stress at which the film fractures. EAB shows the flexibility/extensibility of a film before fracturing. TES values were between 5.7 ± 2 and 22.2 ± 5 N·mm^{-2}, as represented in Figure 6A. No statistical differences were observed between TESof pectin/SLN films and TES of pectin/emulsifier films ($p > 0.05$), indicating that the observed effects are not due to SLN addition but probably due to the emulsifiers and due to a lower amount of pectin network. This could be observed for the TES of CPS film, which had a lower value than Control ($p < 0.05$). The addition of Tween 20 had the most pronounced effect on weakening pectin films, as the lowest TES values were registered in films containing Tween 20. Loaded and free RO had no significant influence on TES ($p > 0.05$).

Pectin created a three-dimensional network during the film-forming process, which resulted in a self-standing film after drying. The film's strength is, among others, determined by the pectin network's density. By adding SLN or emulsifiers, the amount of pectin, and thus, the pectin network, was reduced, and the network was possibly less dense, resulting in a reduced strength of the films. This might be one reason why pectin/SLN films showed a lower TES. In our previous study, protein-stabilized SLN did not influence the TES of protein films, as they acted as an active filler and probably substituted the missing network-forming molecule by being part of the protein network [12]. The reduction of TES by the incorporation of SLN in the present study, especially in PS and PS-RO films, indicates that they were not integrated in the pectin network, thus did not act as active fillers.

A further reason for decreased TES values for pectin/SLN or pectin/emulsifier films might be that emulsifiers acted as plasticizers, thus weakening the films. Small molecules such as Tween 20 can fit between the pectin molecules or interfere with interactions between them, leading to higher molecular mobility, thus increasing the initial plastic effect. This was probably the reason why films containing Tween 20 led to weaker films. The plasticizing effect of emulsifiers in polysaccharide-based films were also reported elsewhere: Tween 20, lecithin, and Span decreased the TES of starch films [48], and Tween 20/40/80 decreased the TES of kappa-carrageenan with the increase of their concentration [50].

EAB was not significantly affected by SLN addition compared to Control ($p > 0.05$), while EAB significantly increased ($p < 0.05$) with the addition of pure emulsifiers without lipids and free RO (Figure 6B). The addition of emulsifiers increased EAB to $7.25\% \pm 1.97\%$ (CTS film) and $12.24\% \pm 2.26\%$ (CPS film)

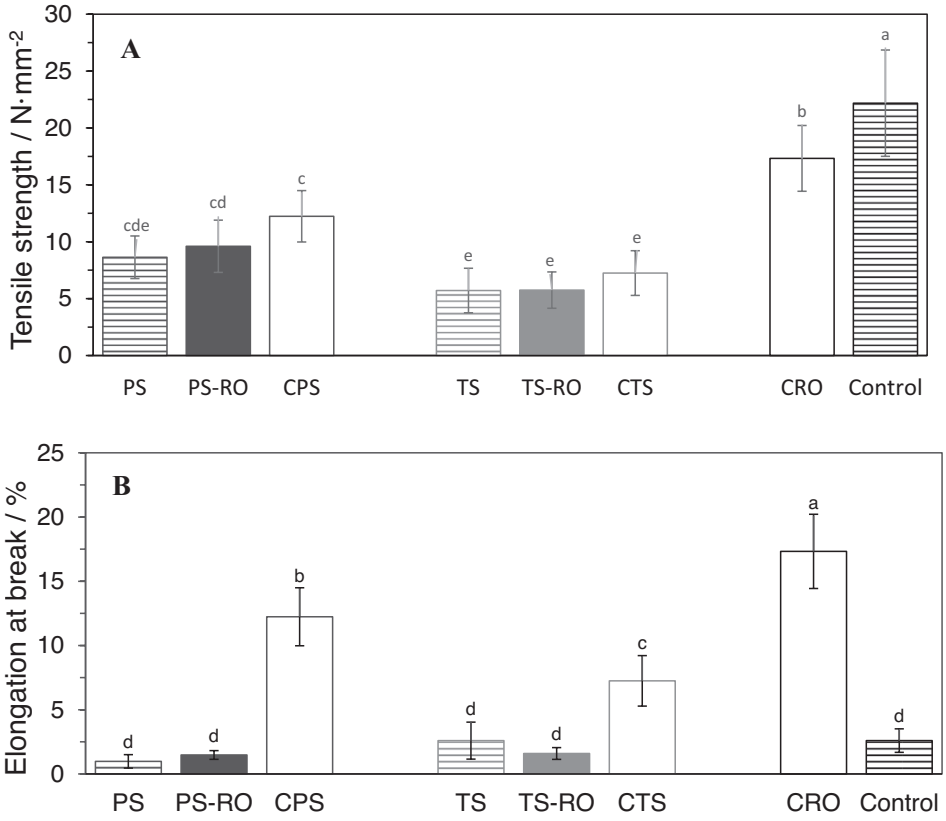

FIGURE 6 | Mechanical properties of pectin films with differently stabilized solid lipid nanoparticles (SLN) that were unloaded or loaded with rosemary oil: (A) tensile strength in N/mm^2; (B) elongation at break in %. Data are expressed as mean ± standard deviation ($n = 3$).

compared to Control (2.60% ± 0.91%). One reason for the low EaB of pectin/SLN films might be that SLN act as "predetermined breaking points". SLN cannot deform, but the matrix deforms due to increased stress, resulting in the matrix breaking at the surface of the particles. A lower EAB in pectin/SLN films compared to their controls, CPS and CTS, could also be explained by the presence of the platelet shape of SLN that adsorb on its surface the emulsifiers [61]. If emulsifiers are used in the presence of lipids, emulsifiers adsorb on the surface and are no longer freely present in the solution, so they cannot act as plasticizers. If no lipid is used, all emulsifiers are freely present or are present as micelles, and can act as plasticizers, as already described by [62]. In this study, the same might hold true for emulsifiers adsorbed onto the platelet shaped SLN, reducing the emulsifiers' availability to interact with the pectin matrix. In summary, the plasticizing effect of the emulsifiers resulting in high EAB values in samples CPS and CTS, is counteracted by the weakening effect of SLN incorporation. In the end, EAB values for pectin/SLN films (PS, PS-RO, TS, TS-RO) equal the EAB of Control. Additionally, the well dispersed SLN helped to distribute local stresses and preserving extensibility. In the case of pectin films containing fluconazole-loaded SLN, small nanoparticles caused higher film integrity and tenacity compared to those containing nanoparticles of a large size [63].

RO-loaded SLN did not affect the EAB of pectin films, probably due to its adsorption on the surface of the SLN. However, free RO significantly increased EABto 17.33% ± 2.89% in CRO film. RO is liquid at room temperature, so it can easily be deformed, increasing the film's extensibility. Similar results were found by Nisar, Wang, Yang, Tian, Iqbal, and Guo [22].

Conventional plastic films have TES values between 6 to 19 (ethylene-vinyl acetate) and 177 (polyethylene terephthalate) N·mm^{-2} and EAB values between 2% and 3% (polystyrene) and 100% (polypropylene), respectively [64]. Therefore, pectin/SLN films had lower mechanical properties than conventional plastic films. In conclusion, adding SLN weakened pectin films without significantly changing their flexibility. By incorporating SLN, TES can be modulated, but not the EAB of films.

3.2.6 | Dynamic Mechanical Analysis (DMA)

According to an improved WVP, pectin/SLN films could be applied to the ready-to-eat food products with a lower water content after the cooking process (e.g., fried/grilled meat). In general, ready-to-eat food products are heated before eat. Therefore, in this study, DMA was used to evaluate the rheological properties of materials and the glass transition profile of pectin films between 30°C and 90°C.

Representative curves of the storage modulus (G′) are presented in Figure 7. G′ indicates the energy storage capacity and is related to the stiffness of films. The loss modulus (G″) represents the viscous characteristics of films and the heat dissipated by the substance as a result of molecular motion (damping) (Figure S6). In this study, all samples had G′ higher than G″, indicating that all films featured a viscoelastic solid profile with a solid-like structure throughout the entire temperature range [65].

Control film had the highest stiffness until 90°C, while the addition of SLN, emulsifiers, and RO decreased the stiffness

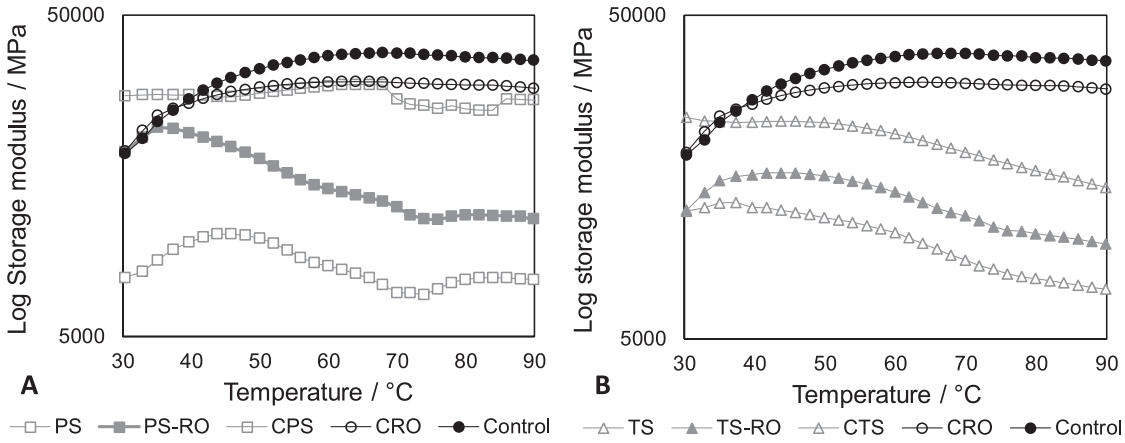

FIGURE 7 | Storage modulus (G′): (A) pectin films with pectin-stabilized SLN. (B) Pectin films with Tween 20-stabilized SLN.

of pectin films as indicated by a lower storage modulus compared to Control over temperature. Firstly, G′ curves of the Control film tended to increase. This could be attributed to the evaporation of water. Water acts as a plasticizer for polysaccharide films and therefore, its removal makes films firmer. In the 25°C–50°C range, a prominent increase of the G′ curve of pectin films was observed by Norcino, de Oliveira, Moreira, Marconcini and Mattoso [66]. The addition of RO directly into the film (sample CRO) reduced G′ only slightly. Moreover, there are differences to be observed between the control samples with added emulsifiers: Apparently, the addition of sucrose palmitate and lecithin did not have a strong impact on film stiffness. The curve of CPS (Figure 7A) shows comparable G′ values as the curves of Control and CRO. In contrast, CTS (Figure 7B), the control sample containing Tween 20, shows much lower G′ values than Control, indicating a much lower film stiffness probably caused by the plasticizing effect of Tween 20. In all cases, SLN reduced the stiffness of the films. However, this effect was more pronounced for pectin-stabilized SLN (compare PS and PS-RO to CPS in Figure 7A) than for SLN stabilized by Tween 20 (compare TS and TS-RO to CTS in Figure 7B). This means that the weakening effect of SLN (= SLN serving as inactive fillers) can also be seen in DMA. However, this effect is less pronounced for TS and TS-RO because the overall weakening effect of Tween 20 is dominating. Finally, there is a difference in the film stiffness between samples containing SLN and SLN loaded with RO. PS and TS show lower G' values than PS-RO and TS-RO. This is because in PS-RO and TS-RO, part of the fat phase is liquid, and thus the effect of "predetermined breaking points" is less pronounced.

Additionally, when analyzing the curves in more detail, the G′ curves of all the samples containing SLN showed several slope changes. For pectin/SLN films, a first peak in G′ was observed around 40°C. Then, G′ decreased in PS and PS-RO until a second peak occurred at a temperature above 65°C (Figure 7A). TS and TS-RO did not show a second peak, but instead, a gentle shoulder was observed between 60°C and 70°C (Figure 7B). These changing points at intermediate temperatures indicated transitions that may correspond to changes on the molecular level, such as changes in the conformation of the pectin or the melting of lipids and emulsifiers. A decrease of G′ curves around 40°C was also reported in protein/SLN films. This tendency was attributed to the melting of the SLN mixture [12].

The melting point of Tween 20 and sucrose palmitate stabilized SLN was already determined and was in the range of 45°C–60°C [67]. Gao, Mao and Meng [68] found a sucrose palmitate peak at about 50°C–70°C in sucrose palmitate-stabilized anhydrous milk fat emulsions. This drop was attributed to the melting point of sucrose palmitate and the melted interfacial crystal, resulting in the change of rheological properties. Tween 20 has a cloud point between 40°C and 80°C, which depends on concentration, solvent, and the presence of other substances [69]. Lecithin has a melting point above 120°C [70] and does not affect the melting point of triglyceride nanoparticles [71]. Therefore, the first transition in all pectin/SLN films at about 40°C could be explained by SLN disintegration due to lipids' melting points. The second transition, above 65°C, could be attributed to the melting point of pectin and sucrose palmitate, thus leading to the onset of entire molecular motion [7]. This is supported by the facts that samples without SLN do not show the first peak in G′ and that CPS showed a specific drop in G′ above 65°C. The absence of a second peak in TS and TS-RO corresponds to the slope of G′ in CTS. It can be seen that the G′ behavior of these samples is dominated by the emulsifier Tween 20. In conclusion, SLN influenced the thermal stability of pectin films due to the disintegration at higher temperatures of emulsifiers and lipids, thus leading to weaker films than the Control.

4 | Conclusion

The current work represents a preliminary material-design and characterization study of pectin/SLN films intended as a food-contact packaging system. Pectin-stabilized SLN showed larger-sized nanoparticles with a more negative ZP and a higher encapsulation efficiency compared to Tween 20-stabilized SLN ($p < 0.05$). Mechanical, thermal, and water barrier properties of pectin films were differently affected by SLN, whether stabilized by pectin or Tween 20. Instead, rosemary oil-loaded SLN had no significant effect on pectin films' properties compared to unloaded SLN ($p < 0.05$). According to SEM images, heterogeneities or aggregates were not observed, indicating a

homogeneous SLN in the pectin matrix. The WVP of pectin films decreased upon SLN incorporation, thus improving the moisture barrier of pectin films by up to 92%. SLN reduced the hydrophilicity of pectin films and led to the formation of tortuous paths, slowing down the diffusion of water molecules through the films. In terms of mechanical properties, no significant differences were observed for elongation at break, while tensile strength was decreased up to 74% due to SLN incorporation ($p < 0.05$). Thereby, SLN acted as a weakener in pectin films, rather than a reinforcement. The low initial water barrier of pectin films was improved by SLN addition, however, at the expense of reduced mechanical performance. Nevertheless, the mechanical properties of pectin/SLN films still seem suitable for food packaging material. The enhanced WVP and additional functionality by RO make them highly interesting as active packaging for ready-to-eat food products with low water content. However, the limitations of this study are acknowledged. The complex interactions among pectin, RO, and the encapsulation system may influence the overall performance of developed packaging material. Therefore, future research should focus on food-contact safety evaluations, including migration, cytotoxicity, and oil resistance, to further validate the applicability of pectin/RO-SLN films for real food packaging applications.

Acknowledgments

The authors thank the team from the Institute for Food and Bioprocess Engineering of Max Rubner-Institute (Karlsruhe, Germany), especially Karin Heck, Christian Geuter, Birgit Hetzer, Simone Brümmer, and Gunilla Breutmann. We also thank the team from the Department of Food Process Engineering of Karlsruhe Institute for Technology (Karlsruhe, Germany) for their continued support, fruitful discussion, and excellent help. The authors thank Simon Elemer for his support with the antimicrobial assay. Open Access funding enabled and organized by Projekt DEAL.

Funding

The financial support from the German Federal Environmental Foundation (Deutsche Bundesstiftung Umwelt, 30021/951-46), together with the financial support from the Romanian Ministry of Research, Development, and Innovation, CNCS-UEFISCDI, project number 57PHE February 6, 2024 (PN-IV-P8-8.1-PRE-HE-ORG-2023-0146) is gratefully acknowledged.

Conflicts of Interest

The authors declare no conflicts of interest.

Data Availability Statement

Data will be made available on request.

References

1. S. A. A. Mohamed, M. El-Sakhawy, and M. A. El-Sakhawy, "Polysaccharides, Protein and Lipid -Based Natural Edible Films in Food Packaging: A Review," *Carbohydrate Polymers* 238 (2020): 116178, https://doi.org/10.1016/j.carbpol.2020.116178.

2. U. S. Schmidt, L. Schütz, and H. P. Schuchmann, "Interfacial and Emulsifying Properties of Citrus Pectin: Interaction of pH, Ionic Strength and Degree of Esterification," *Food Hydrocolloids* 62 (2017): 288–298, https://doi.org/10.1016/j.foodhyd.2016.08.016.

3. J. R. Nastasi, V. Kontogiorgos, V. D. Daygon, and M. A. Fitzgerald, "Pectin-Based Films and Coatings With Plant Extracts as Natural Preservatives: A Systematic Review," *Trends in Food Science and Technology* 120 (2022): 193–211, https://doi.org/10.1016/j.tifs.2022.01.014.

4. G. A. Martău, M. Mihai, and D. C. Vodnar, "The Use of Chitosan, Alginate, and Pectin in the Biomedical and Food Sector—Biocompatibility, Bioadhesiveness, and Biodegradability," *Polymers* 11, no. 11 (2019): 1837, https://doi.org/10.3390/polym11111837.

5. V. A. Kumar, M. Hasan, S. Mangaraj, M. Pravitha, D. K. Verma, and P. P. Srivastav, "Trends in Edible Packaging Films and Its Prospective Future in Food: A Review," *Applied Food Research* 2, no. 1 (2022): 100118, https://doi.org/10.1016/j.afres.2022.100118.

6. L. Atarés and A. Chiralt, "Essential Oils as Additives in Biodegradable Films and Coatings for Active Food Packaging," *Trends in Food Science and Technology* 48 (2016): 51–62, https://doi.org/10.1016/j.tifs.2015.12.001.

7. M. L. Fishman, D. R. Coffin, C. I. Onwulata, and J. L. Willett, "Two Stage Extrusion of Plasticized Pectin/Poly(Vinyl Alcohol) Blends," *Carbohydrate Polymers* 65, no. 4 (2006): 421–429, https://doi.org/10.1016/j.carbpol.2006.01.032.

8. T. H. Shellhammer and J. M. Krochta, "Whey Protein Emulsion Film Performance as Affected by Lipid Type and Amount," *Journal of Food Science* 62, no. 2 (1997): 390–394, https://doi.org/10.1111/j.1365-2621.1997.tb04008.x.

9. P. Simić and N. P. Ulrih, "Rosemary Essential Oil as a Natural Additive in Food Industry: Recent Developments in Encapsulation Techniques," *Foods* 15, no. 5 (2026): 893, https://doi.org/10.3390/foods15050893.

10. A. Katopodi and A. Detsi, "Solid Lipid Nanoparticles and Nanostructured Lipid Carriers of Natural Products as Promising Systems for Their Bioactivity Enhancement: The Case of Essential Oils and Flavonoids," *Colloids and Surfaces A: Physicochemical and Engineering Aspects* 630 (2021): 127529, https://doi.org/10.1016/j.colsurfa.2021.127529.

11. M. Farahani, F. Shahidi, F. T. Yazdi, and A. Ghaderi, "Antimicrobial and Antioxidant Effects of an Edible Coating of *Lepidium sativum* Seed Mucilage and *Satureja hortensis* L. Essential Oil in Uncooked Lamb Meat," *Food Control* 158 (2024): 158110240, https://doi.org/10.1016/j.foodcont.2023.110240.

12. V. Wiedenmann, K. Oehlke, U. van der Schaaf, H. M. Koivula, K. S. Mikkonen, and H. P. Karbstein, "Emulsifier Composition of Solid Lipid Nanoparticles (SLN) Affects Mechanical and Barrier Properties of SLN-Protein Composite Films," *Journal of Food Science* 84, no. 12 (2019): 3642–3652, https://doi.org/10.1111/1750-3841.14950.

13. S. Huang, Y. Zhang, Q. Chen, et al., "Pectin Based Gels and Their Advanced Application in Food: From Hydrogel to Emulsion Gel," *Food Hydrocolloids* 160 (2025): 110841, https://doi.org/10.1016/j.foodhyd.2024.110841.

14. J. Xie, Y. Zhang, S. Klomklao, and B. K. Simpson, "Pectin From Plantain Peels: Green Recovery for Transformation Into Reinforced Packaging Films," *Waste Management* 161 (2023): 225–233, https://doi.org/10.1016/j.wasman.2023.02.035.

15. A. McDaniel, B. Tonyali, U. Yucel, and V. Trinetta, "Formulation and Development of Lipid Nanoparticle Antifungal Packaging Films to Control Postharvest Disease," *Journal of Agriculture and Food Research* 1 (2019): 100013, https://doi.org/10.1016/j.jafr.2019.100013.

16. F. Cruces, M. G. García, and N. A. Ochoa, "Reduction of Water Vapor Permeability in Food Multilayer Biopackaging by Epitaxial Crystallization of Beeswax," *Food and Bioprocess Technology* 14, no. 7 (2021): 1244–1255, https://doi.org/10.1007/s11947-021-02628-9.

17. Y. Ma, W. Li, S. Tan, and Q. Yu, "Characterization and Application of Citrus Pectin Composite Film Containing Rosemary (*Rosmarinus officinalis* L.) Essential Oil for Improving Storage of Chilled Beef," *Journal of*

the Science of Food and Agriculture 105, no. 4 (2025): 2390–2402, https://doi.org/10.1002/jsfa.14009.

18. R. Akhter, F. A. Masoodi, and T. A. Wani, "Chitosan, Gelatin and Pectin Based Bionanocomposite Films With Rosemary Essential Oil as an Active Ingredient for Future Foods," *International Journal of Biological Macromolecules* 272, no. Pt 1 (2024): 132813, https://doi.org/10.1016/j.ijbiomac.2024.132813.

19. S. Safaeian Laein, F. Mohajer, A. Khanzadi, et al., "Effect of Alginate Coating Activated by Solid Lipid Nanoparticles Containing Zataria Multiflora Essential Oil on Chicken Fillet's Preservation," *Food Chemistry* 446 (2024): 138816, https://doi.org/10.1016/j.foodchem.2024.138816.

20. P. Fincheira, J. Espinoza, M. Levio-Raiman, et al., "Formulation of Essential Oils-Loaded Solid Lipid Nanoparticles-Based Chitosan/PVA Hydrogels to Control the Growth of Botrytis Cinerea and Penicillium Expansum," *International Journal of Biological Macromolecules* 270, no. Pt 1 (2024): 132218, https://doi.org/10.1016/j.ijbiomac.2024.132218.

21. J. Xue, T. Wang, Q. Hu, M. Zhou, and Y. Luo, "A Novel and Organic Solvent-Free Preparation of Solid Lipid Nanoparticles Using Natural Biopolymers as Emulsifier and Stabilizer," *International Journal of Pharmaceutics* 531, no. 1 (2017): 59–66, https://doi.org/10.1016/j.ijpharm.2017.08.066.

22. T. Nisar, Z. C. Wang, X. Yang, Y. Tian, M. Iqbal, and Y. Guo, "Characterization of Citrus Pectin Films Integrated With Clove Bud Essential Oil: Physical, Thermal, Barrier, Antioxidant and Antibacterial Properties," *International Journal of Biological Macromolecules* 106 (2018): 670–680, https://doi.org/10.1016/j.ijbiomac.2017.08.068.

23. G. Granata, S. Stracquadanio, M. Leonardi, et al., "Essential Oils Encapsulated in Polymer-Based Nanocapsules as Potential Candidates for Application in Food Preservation," *Food Chemistry* 269 (2018): 286–292, https://doi.org/10.1016/j.foodchem.2018.06.140.

24. V. Siracusa, S. Romani, M. Gigli, et al., "Characterization of Active Edible Films Based on Citral Essential Oil, Alginate and Pectin," *Materials* 11, no. 10 (2018): 1980, https://doi.org/10.3390/ma11101980.

25. J. Andrzejewski, K. Grad, W. Wiśniewski, and J. Szulc, "The Use of Agricultural Waste in the Modification of Poly(Lactic Acid)-Based Composites Intended for 3D Printing Applications. The Use of Toughened Blend Systems to Improve Mechanical Properties," *Journal of Composites Science* 5, no. 10 (2021): 253, https://doi.org/10.3390/jcs5100253.

26. H. Almasi, S. Azizi, and S. Amjadi, "Development and Characterization of Pectin Films Activated by Nanoemulsion and Pickering Emulsion Stabilized Marjoram (*Origanum majorana* L.) Essential Oil," *Food Hydrocolloids* 99 (2020): 105338, https://doi.org/10.1016/j.foodhyd.2019.105338.

27. Z. Li, X. Jiang, H. Huang, et al., "Chitosan/Zein Films Incorporated With Essential Oil Nanoparticles and Nanoemulsions: Similarities and Differences," *International Journal of Biological Macromolecules* 208 (2022): 983–994, https://doi.org/10.1016/j.ijbiomac.2022.03.200.

28. T. Wang, X. Ma, Y. Lei, and Y. Luo, "Solid Lipid Nanoparticles Coated With Cross-Linked Polymeric Double Layer for Oral Delivery of Curcumin," *Colloids and Surfaces. B, Biointerfaces* 148 (2016): 1–11, https://doi.org/10.1016/j.colsurfb.2016.08.047.

29. M. Miranda, M. T. Cruz, C. Vitorino, and C. Cabral, "Nanostructuring Lipid Carriers Using Ridolfia Segetum (L.) Moris Essential Oil," *Materials Science & Engineering. C, Materials for Biological Applications* 103 (2019): 109804, https://doi.org/10.1016/j.msec.2019.109804.

30. E. B. Souto, P. Severino, C. Marques, et al., "*Croton argyrophyllus* Kunth Essential Oil-Loaded Solid Lipid Nanoparticles: Evaluation of Release Profile, Antioxidant Activity and Cytotoxicity in a Neuroblastoma Cell Line," *Sustainability* 12, no. 18 (2020): 7697, https://doi.org/10.3390/su12187697.

31. B. Bindereif, H. P. Karbstein, K. Zahn, and U. S. van der Schaaf, "Effect of Conformation of Sugar Beet Pectin on the Interfacial and Emulsifying Properties," *Foods* 11, no. 2 (2022): 214, https://doi.org/10.3390/foods11020214.

32. T. R. Wang, M. Bae, J. Y. Lee, and Y. C. Luo, "Solid Lipid-Polymer Hybrid Nanoparticles Prepared With Natural Biomaterials: A New Platform for Oral Delivery of Lipophilic Bioactives," *Food Hydrocolloids* 84 (2018): 581–592, https://doi.org/10.1016/j.foodhyd.2018.06.041.

33. T. E. Mungure, S. Roohinejad, A. E. Bekhit, R. Greiner, and K. Mallikarjunan, "Potential Application of Pectin for the Stabilization of Nanoemulsions," *Current Opinion in Food Science* 19 (2018): 72–76, https://doi.org/10.1016/j.cofs.2018.01.011.

34. D. J. McClements, *Food Emulsions: Principles, Practices, and Techniques*, 3rd ed. (CRC Press, 2015).

35. M. Nasseri, S. Golmohammadzadeh, H. Arouiee, M. R. Jaafari, and H. Neamati, "Antifungal Activity of Zataria Multiflora Essential Oil-Loaded Solid Lipid Nanoparticles In-Vitro Condition," *Iranian Journal of Basic Medical Sciences* 19, no. 11 (2016): 1231–1237.

36. F. S. G. Saporito, M. C. Bonferoni, S. Rossi, et al., "Essential Oil-Loaded Lipid Nanoparticles for Wound Healing," *International Journal of Nanomedicine* 13 (2018): 175–186, https://doi.org/10.2147/IJN.S152529.

37. O. A. Attallah, A. Shetta, F. Elshishiny, and W. Mamdouh, "Essential Oil Loaded Pectin/Chitosan Nanoparticles Preparation and Optimization via Box-Behnken Design Against MCF-7 Breast Cancer Cell Lines," *RSC Advances* 10, no. 15 (2020): 8703–8708, https://doi.org/10.1039/c9ra10204c.

38. S. F. Tabatabaeain, E. Karimi, and M. Hashemi, "Satureja Khuzistanica Essential Oil-Loaded Solid Lipid Nanoparticles Modified With Chitosan-Folate: Evaluation of Encapsulation Efficiency, Cytotoxic and Pro-Apoptotic Properties," *Frontier Chemistry* 10 (2022): 904973, https://doi.org/10.3389/fchem.2022.904973.

39. F. Hosseinpour Jajarm, G. Moravvej, M. Modarres Awal, and S. Golmohammadzadeh, "Insecticidal Activity of Solid Lipid Nanoparticle Loaded by Ziziphora Clinopodioides Lam. Against *Tribolium castaneum* (Herbst, 1797) (Coleoptera: Tenebrionidae)," *International Journal of Pest Management* 67, no. 2 (2021): 147–154, https://doi.org/10.1080/09670874.2020.1713420.

40. F. T. Sarıcaoglu and S. Turhan, "Physicochemical, Antioxidant and Antimicrobial Properties of Mechanically Deboned Chicken Meat Protein Films Enriched With Various Essential Oils," *Food Packaging and Shelf Life* 25 (2020): 100527, https://doi.org/10.1016/j.fpsl.2020.100527.

41. S. Mehraj and Y. S. Sistla, "Optimization of Process Conditions for the Development of Pectin and Glycerol Based Edible Films: Statistical Design of Experiments," *Electronic Journal of Biotechnology* 55 (2022): 27–39, https://doi.org/10.1016/j.ejbt.2021.11.004.

42. Z. A. Nur Hanani and A. B. Aelma Husna, "Effect of Different Types and Concentrations of Emulsifier on the Characteristics of Kappa-Carrageenan Films," *International Journal of Biological Macromolecules* 114 (2018): 710–716, https://doi.org/10.1016/j.ijbiomac.2018.03.163.

43. M. Kurek, N. Benbettaieb, M. Scetar, et al., "Novel Functional Chitosan and Pectin Bio-Based Packaging Films With Encapsulated-Waste," *Food Bioscience* 41 (2021): 100980, https://doi.org/10.1016/j.fbio.2021.100980.

44. L. B. Norcino, J. F. Mendes, C. V. L. Natarelli, A. Manrich, J. E. Oliveira, and L. H. C. Mattoso, "Pectin Films Loaded With Copaiba Oil Nanoemulsions for Potential Use as Bio-Based Active Packaging," *Food Hydrocolloids* 106 (2020): 105862, https://doi.org/10.1016/j.foodhyd.2020.105862.

45. J. Vartiainen, T. Tammelin, J. Pere, U. Tapper, and A. Harlin, "Biohybrid Barrier Films From Fluidized Pectin and Nanoclay," *Carbohydrate Polymers* 82, no. 3 (2010): 989–996, https://doi.org/10.1016/j.carbpol.2010.06.031.

46. H. G. R. Younis, H. R. S. Abdellatif, F. Ye, and G. Zhao, "Tuning the Physicochemical Properties of Apple Pectin Films by Incorporating Chitosan/Pectin Fiber," *International Journal of Biological Macromolecules* 159 (2020): 213–221, https://doi.org/10.1016/j.ijbiomac.2020.05.060.

47. F. F. Shih, K. W. Daigle, and E. T. Champagne, "Effect of Rice Wax on Water Vapour Permeability and Sorption Properties of Edible Pullulan Films," *Food Chemistry* 127, no. 1 (2011): 118–121, https://doi.org/10.1016/j.foodchem.2010.12.096.

48. M. Rodríguez, J. Osés, K. Ziani, and J. I. Maté, "Combined Effect of Plasticizers and Surfactants on the Physical Properties of Starch Based Edible Films," *Food Research International* 39, no. 8 (2006): 840–846, https://doi.org/10.1016/j.foodres.2006.04.002.

49. T. Schmidts, D. Dobler, C. Nissing, and F. Runkel, "Influence of Hydrophilic Surfactants on the Properties of Multiple W/O/W Emulsions," *Journal of Colloid and Interface Science* 338, no. 1 (2009): 184–192, https://doi.org/10.1016/j.jcis.2009.06.033.

50. B. Saberi, S. Chockchaisawasdee, J. B. Golding, C. J. Scarlett, and C. E. Stathopoulos, "Development of Biocomposite Films Incorporated With Different Amounts of Shellac, Emulsifier, and Surfactant," *Food Hydrocolloids* 72 (2017): 174–184, https://doi.org/10.1016/j.foodhyd.2017.05.042.

51. B.-E. Teleky, L. Mitrea, D. Plamada, et al., "Development of Pectin and Poly(Vinyl Alcohol)-Based Active Packaging Enriched With Itaconic Acid and Apple Pomace-Derived Antioxidants," *Antioxidants* 11, no. 9 (2022): 1729, https://doi.org/10.3390/antiox11091729.

52. J. Milsmann, K. Oehlke, K. Schrader, R. Greiner, and A. Steffen-Heins, "Fate of Edible Solid Lipid Nanoparticles (SLN) in Surfactant Stabilized o/w Emulsions. Part 1: Interplay of SLN and Oil Droplets," *Colloids and Surfaces A, Physicochemical and Engineering Aspects* 558 (2018): 615–622, https://doi.org/10.1016/j.colsurfa.2017.05.073.

53. V. Wiedenmann, K. Oehlke, U. van der Schaaf, B. Hetzer, R. Greiner, and H. P. Karbstein, "Impact of the Incorporation of Solid Lipid Nanoparticles on β-Lactoglobulin Gel Matrices," *Food Hydrocolloids* 84 (2018): 498–507, https://doi.org/10.1016/j.foodhyd.2018.06.007.

54. M. Abdollahi, M. Rezaei, and G. Farzi, "A Novel Active Bionanocomposite Film Incorporating Rosemary Essential Oil and Nanoclay Into Chitosan," *Journal of Food Engineering* 111, no. 2 (2012): 343–350, https://doi.org/10.1016/j.jfoodeng.2012.02.012.

55. K. Yano, A. Usuki, and A. Okada, "Synthesis and Properties of Polyimide-Clay Hybrid Films," *Journal of Polymer Science Part A-Polymer Chemistry* 35, no. 11 (1997): 2289–2294, https://doi.org/10.1002/(Sici)1099-0518(199708)35:11<2289::Aid-Pola20>3.0.Co;2-9.

56. S. K. Zhang, Z. Y. He, F. Z. Xu, et al., "Enhancing the Performance of Konjac Glucomannan Films Through Incorporating Zein-Pectin Nanoparticle-Stabilized Oregano Essential Oil Pickering Emulsions," *Food Hydrocolloids* 130 (2022): 107222, https://doi.org/10.1016/j.foodhyd.2022.107724.

57. K. Norajit, K. M. Kim, and G. H. Ryu, "Comparative Studies on the Characterization and Antioxidant Properties of Biodegradable Alginate Films Containing Ginseng Extract," *Journal of Food Engineering* 98, no. 3 (2010): 377–384, https://doi.org/10.1016/j.jfoodeng.2010.01.015.

58. K. Ziani, J. Oses, V. Coma, and J. I. Maté, "Effect of the Presence of Glycerol and Tween 20 on the Chemical and Physical Properties of Films Based on Chitosan With Different Degree of Deacetylation," *LWT- Food Science and Technology* 41, no. 10 (2008): 2159–2165, https://doi.org/10.1016/j.lwt.2007.11.023.

59. S.-I. Hong, L.-F. Wang, and J.-W. Rhim, "Preparation and Characterization of Nanoclays-Incorporated Polyethylene/Thermoplastic Starch Composite Films With Antimicrobial Activity," *Food Packaging and Shelf Life* 31 (2022): 100784, https://doi.org/10.1016/j.fpsl.2021.100784.

60. D. J. da Silva, M. M. de Oliveira, S. H. Wang, D. J. Carastan, and D. S. Rosa, "Designing Antimicrobial Polypropylene Films With Grape Pomace Extract for Food Packaging," *Food Packaging and Shelf Life* 34 (2022): 100929, https://doi.org/10.1016/j.fpsl.2022.100929.

61. H. Rostamzad, S. Y. Paighambari, B. Shabanpour, S. M. Ojagh, and S. M. Mousavi, "Improvement of Fish Protein Film With Nanoclay and Transglutaminase for Food Packaging," *Food Packaging and Shelf Life* 7 (2016): 1–7, https://doi.org/10.1016/j.fpsl.2015.10.001.

62. T. I. Oliveira, L. Zea-Redondo, G. K. Moates, et al., "Pomegranate Peel Pectin Films as Affected by Montmorillonite," *Food Chemistry* 198 (2016): 107–112, https://doi.org/10.1016/j.foodchem.2015.09.109.

63. N. Hirun, J. Mahadlek, S. Limmatvapirat, et al., "Fabrication and Characterization of Pectin Films Containing Solid Lipid Nanoparticles for Buccal Delivery of Fluconazole," *International Journal of Molecular Sciences* 25, no. 10 (2024): 5413, https://doi.org/10.3390/ijms25105413.

64. L. Bastarrachea, S. Dhawan, and S. S. Sablani, "Engineering Properties of Polymeric-Based Antimicrobial Films for Food Packaging: A Review," *Food Engineering Reviews* 3, no. 2 (2011): 79–93, https://doi.org/10.1007/s12393-011-9034-8.

65. M. A. Bashir, "Use of Dynamic Mechanical Analysis (DMA) for Characterizing Interfacial Interactions in Filled Polymers," *Solids* 2, no. 1 (2021): 108–120, https://doi.org/10.3390/solids2010006.

66. L. B. Norcino, J. E. de Oliveira, F. K. V. Moreira, J. M. Marconcini, and L. H. C. Mattoso, "Rheological and Thermo-Mechanical Evaluation of Bio-Based Chitosan/Pectin Blends With Tunable Ionic Cross-Linking," *International Journal of Biological Macromolecules* 118, no. Pt B (2018): 1817–1823, https://doi.org/10.1016/j.ijbiomac.2018.07.027.

67. K. Oehlke, D. Behsnilian, E. Mayer-Miebach, P. G. Weidler, and R. Greiner, "Edible Solid Lipid Nanoparticles (SLN) as Carrier System for Antioxidants of Different Lipophilicity," *PLoS One* 12, no. 2 (2017): e0171662, https://doi.org/10.1371/journal.pone.0171662.

68. Y. Gao, J. Mao, and Z. Meng, "Tracing Distribution and Interface Behavior of Water Droplets in W/O Emulsions With Fat Crystals," *Food Research International* 163 (2023): 112215, https://doi.org/10.1016/j.foodres.2022.112215.

69. J. Chawla and R. K. Mahajan, "Cloud Point Studies of Tween and Glycol in the Presence of Salts," *Journal of Dispersion Science and Technology* 32, no. 6 (2011): 822–827, https://doi.org/10.1080/01932691.2010.488138.

70. L. J. Han, L. Li, L. Zhao, et al., "Rheological Properties of Organogels Developed by Sitosterol and Lecithin," *Food Research International* 53, no. 1 (2013): 42–48, https://doi.org/10.1016/j.foodres.2013.03.039.

71. M. A. Schubert, B. C. Schicke, and C. C. Muller-Goymann, "Thermal Analysis of the Crystallization and Melting Behavior of Lipid Matrices and Lipid Nanoparticles Containing High Amounts of Lecithin," *International Journal of Pharmaceutics* 298, no. 1 (2005): 242–254, https://doi.org/10.1016/j.ijpharm.2005.04.014.

Supporting Information

Additional supporting information can be found online in the Supporting Information section. **Figure S1:** Disk diffusion test. PS, pectin/pectin-stabilized SLN film forming solution; PS-RO, pectin/rosemary oil loaded pectin-stabilized SLN film forming solution; TS, pectin/Tween 20-stabilized SLN film forming solution; TS-RO, pectin/rosemary oil-loaded Tween 20-stabilized SLN film forming solution. **Figure S2:** The opacity of pectin films containing unloaded (PS, TS) or rosemary oil-loaded (PS-RO, TS-RO) SLN, emulsifiers (CPS, CTS) and rosemary oil (CRO). Data are expressed as mean ± standard deviation ($n = 9$). **Figure S3:** Curves of theoretical water sorption isotherm based on each raw material's water sorption contribution. **Figure S4:** Water sorption isotherm of raw materials. Data are expressed as mean ± SD ($n = 3$). **Figure S5:** Correlation between water sorption isotherm at 0.84 a_w and the content of hydrophilic materials (pectin, glycerol and $CaCl_2$)

in dry mass of films. **Figure S6:** Log loss modulus (G″) of pectin/solid lipid nanoparticles (SLN) films. PS, pectin/pectin-stabilized SLN film; PS-RO, pectin/rosemary oil loaded pectin-stabilized SLN film; CPS, pectin/emulsifiers used in PS (lecithin and sucrose palmitate) film; TS, pectin/Tween 20-stabilized SLN film; TS-RO, pectin/rosemary oil-loaded Tween 20-stabilized SLN film; CTS, pectin/emulsifiers used in TS (lecithin, sucrose palmitate, Tween 20) film; CRO, pectin/rosemary oil film; Control, pectin film. **Table S1:** Thickness of pectin films with differently stabilized solid lipid nanoparticles (SLN) that were unloaded or loaded with rosemary oil.